10-1-2011

Innovative Manufacturing Process for Defect Free, Affordable, High Pressure, Thin Walled, Hydraulic Tubing

W. Miranda

G. Takiguchi

T. Shimabukuro

L. McLennan

C. Agajanian

See next page for additional authors

Authors
W. Miranda, G. Takiguchi, T. Shimabukuro, L. McLennan, C. Agajanian, L. Quintero, D. Mismar, J. Abdulla, C. Andrews, M. Hahn, E. Fodran, E. W. Lee, H. Garmestani, R. D. Conner, D. Brick, J. Ogren, and Omar S. Es-Said

JMEPEG (2011) 20:1206–1218
DOI: 10.1007/s11665-010-9736-8

Innovative Manufacturing Process for Defect Free, Affordable, High Pressure, Thin Walled, Hydraulic Tubing

W. Miranda, G. Takiguchi, T. Shimabukuro, L. McLennan, C. Agajanian, L. Quintero, D. Mismar, J. Abdulla, C. Andrews, M. Hahn, E. Fodran, E.W. Lee, H. Garmestani, R.D. Conner, D. Brick, J. Ogren, and O.S. Es-Said

(Submitted April 20, 2010; in revised form July 25, 2010)

Various thermo-mechanical processes were performed on a standard and a low oxygen content Ti-6Al-4V alloy. Testing was performed to determine whether it was possible to achieve a combination of tensile properties comparable to those of Ti-3Al-2.5V by means of cold working and annealing Ti-6Al-4V from a thickness of 0.671 cm (0.264 in.) to that between 0.081 and 0.094 cm (0.032-0.037 in.), which had never been carried out before. The resulting mechanical properties of this study were compared to the mechanical properties of Ti-3Al-2.5V to determine whether Ti-6Al-4V could be used as a suitable replacement for hydraulic tubing applications. The optimum results were achieved with 10-15% cold work and annealing at 750 °C (1382 °F) for 2 h between cold work reductions in thickness. It was concluded that Ti-6Al-4V was a suitable replacement for Ti-3Al-2.5V for hydraulic tubing with an increase in ultimate and yield strengths, but with a slight sacrifice of 5-10% elongation.

Keywords cold rolling and annealing, optimization of mechanical properties, Ti-6Al-4V

1. Introduction

The V-22 Osprey is a Navy-operated joint service, multi-mission, military tilt rotor aircraft with both a vertical takeoff and landing, and short takeoff and landing capabilities. The V-22 was developed by Bell Helicopter Textron, which manufactures it in partnership with Boeing helicopters, and is defined by the FAA as a model of power lift aircraft (Ref 1, 2). As early as December 2000, the Osprey had experienced failures directly associated with its titanium hydraulic lines. Program officials grounded the fleet citing hydraulic line defects. It was later found that the current titanium tubing used in the Osprey was the reason behind the reported failures (Ref 3-7).

The tubing currently used for the Osprey's hydraulic lines is manufactured using Ti-3Al-2.5V. This alloy is classified as an alpha-beta alloy and is generally used in the cold-worked and stress-relieved conditions. Typical tensile properties of Ti-3Al-2.5V include yield strengths between 517 and 579 MPa (75-84 ksi), tensile strengths of 620-648 MPa (90-94 ksi), and an elongation between 15 and 29% in the cold-worked and stress-relieved conditions (Ref 8). Ti-3Al-2.5V also has a high specific strength which justifies its use in aircraft hydraulic lines (Ref 9, 10). Since strength-related failures occurred in the Ti-3Al-2.5V-based tubing, the use of another stronger alloy was explored.

Ti-6Al-4V was considered as a possible replacement for Ti-3Al-2.5V since it offered a large increase in strength. Disadvantages to Ti-6Al-4V include difficulty in forming at room temperature and low ductility (compared to Ti-3Al-2.5V). Ti-6Al-4V has poor room-temperature shaping and forming characteristics compared to steel and aluminum and is primarily used in the annealed condition. Ti-6Al-4V is not easily straightened when cold worked due to spring-back and resistance to strengthening at room temperature. This is why elevated-temperature forming is usually necessary (Ref 10, 11).

Tubings like those that failed in the Osprey are formed in a process called tube pilgering. Since such forming equipment was not available at the time of performing this research work, a thermomechanical processing scheme was devised, which would best replicate the pilgering process. Tube pilgering is a deformation process, which is usually performed at an elevated temperature, similar to hot rolling. Materials formed this way are often used in the annealed condition. To replicate this process, a cold work and annealing schedule was created in this study. New forms of tube forming include cold pilgering, which causes deformation of the material at room temperature, similar to the cold rolling taking place during this experiment's thermo-mechanical processing steps (Ref 12).

To achieve specific combinations of material properties such as strength, ductility, toughness, and thermal stability, annealing heat treatments are done. Annealing can also be used to relieve stresses in a material. To obtain high strength with adequate ductility, it is generally necessary to heat treat the alloy in the alpha-beta field below the beta transus of the alloy (Ref 9). The effects of slow cooling Ti-6Al-4V cause equiaxed alpha grains to form. This provides good ductility and formability while

W. Miranda, G. Takiguchi, T. Shimabukuro, L. McLennan, C. Agajanian, L. Quintero, D. Mismar, J. Abdulla, C. Andrews, J. Ogren, and **O.S. Es-Said**, Mechanical Engineering Department, Loyola Marymount University, Los Angeles, CA 90045; **M. Hahn** and **E. Fodran**, Northrop Grumman, Air Combat Systems, El Segundo, CA 90245; **E.W. Lee**, Naval Air Systems Command, Naval Air Warfare Center, Patuxent River, MD 20670; **H. Garmestani**, Materials Science and Engineering, Georgia Institute of Technology, Atlanta, GA 30332; **R.D. Conner**, California State University Northridge, 18111 Nordhoff Street, Northridge, CA 91330; and **D. Brick**, Fasteel Corporation, Anaheim, CA 92805. Contact e-mail: oessaid@lmu.edu.

making it difficult for fatigue cracks to nucleate. The effects of faster cooling produce an acicular (basket weave) alpha phase. Fatigue cracks may nucleate but must follow the path along the tortuous boundaries. Ti-6Al-4V can be air cooled from the annealing temperature without impairing its stability, but furnace cooling may result in the formation of Ti_3Al (Ref 9).

In addition to testing a standard version of the Ti-6Al-4V alloy, an ELI (extra low interstitial) version was also tested. The ELI version of Ti-6Al-4V contains less oxygen compared with the standard material. Oxygen is the most important interstitial solute in titanium alloys because it strongly influences the microstructural and mechanical properties. Most commercial titanium alloys contain concentrations between 0.10 and 0.2 wt.% oxygen. Interstitial oxygen can markedly affect the fracture toughness and uniaxial tensile properties of titanium alloys. Oxygen hardens titanium alloys (Ref 13, 14).

The objective of this study is to reduce the thickness of a Ti-6Al-4V to be between 0.081 and 0.094 cm (0.032-0.037 in.) by means of cold rolling with intermediate annealing and to achieve a yield strength greater than 517-579 MPa (75-84 ksi) and an ultimate strength greater than 620-648 MPa (90-94 ksi) with an elongation near 15%. This would validate Ti-6Al-4V as suitable material to be used as a substitute versus Ti-3Al-2.5V.

Table 1 Chemical composition of standard Ti-6Al-4V alloy 0.65-cm (0.256 in.) thickness

Element	Al	V	Fe	Y	C	O	N	Ti
Results	6.19	3.78	0.19	<50 ppm	0.02	0.13	0.005	Bal

Table 2 Chemical composition of standard Ti-6Al-4V alloy 0.254-cm (0.100 in.) thickness

Element	Al	V	Fe	Y	C	O	H	N	Ti
Results	6.20	3.80	0.18	0.001	0.01	0.13	0.0039	0.01	Bal
Max	6.75	4.50	0.30	0.005	0.08	0.20	0.0125	0.05	
Min	5.50	3.50							

2. Experimental

Ti-6Al-4V material was received from Trans World Alloys Co. The chemical composition of the standard and ELI plate materials can be seen in Table 1-3. The material tensile test specification sheets for the standard and ELI Ti-6Al-4V plates are shown in Table 4-6.

Due to the lack of adequate information regarding the cold rolling and annealing of Ti-6Al-4V, separate phases of thermomechanical processing testing were performed to provide sufficient information on cold rolling and annealing parameters of the alloy. The first two stages utilized a Stanat FX-200, 6 in. cold rolling mill. However, due to the rolling machine failure, the third and fourth stage of processing used a Stanat CX-100, 4 in. cold rolling mill, and the final stage used a LOMA rolling mill. Annealing was performed using Thermolyne Series 9000 ovens and a Thermolyne Model 30400 furnace.

The first stage of processing involved testing various thickness reductions coupled with intermediate annealing

Table 3 Chemical composition of ELI Ti-6Al-4V alloy 0.554-cm (0.218 in.) thickness

Element	Al	V	Fe	Y	C	O	Cu	Zr	Mn	Sn	Ni	Cr	Mo
Results	5.98	3.74	0.20	<0.01			<0.01	<0.01	<0.01	<0.01	0.01	0.04	<0.01
Max	6.50	4.50	0.25										
Min	5.50	3.50											

Table 4 Specification sheet of standard Ti-6Al-4V alloy 0.65-cm (0.256 in.) thickness used in the initial stages

Sample identification	Thickness, cm (in.)	Yield strength, MPa (ksi)	Tensile strength, MPa (ksi)	Elongation, %
Longitudinal	0.635 (0.250)	943/952 (137/138)	1001/1008 (145/146)	10/13
Transverse	0.635 (0.250)	982/996 (142/144)	1035/1041 (150/151)	11/13

Table 5 Specification sheet of standard Ti-6Al-4V alloy 0.254-cm (0.100 in.) thickness used in the final stages

Sample identification	Thickness, cm (in.)	Yield strength, MPa (ksi)	Tensile strength, MPa (ksi)	Elongation, %
Longitudinal	0.262 (0.1031)	944 (137)	1020 (148)	12.0
Transverse	0.271 (0.1067)	985 (143)	1020 (148)	13.0
Minimum		868 (126)	923 (134)	10.0

Table 6 Specification sheet of ELI Ti-6Al-4V alloy 0.554-cm (0.218 in.) thickness

Sample identification	Thickness, cm (in.)	Yield strength, MPa (ksi)	Tensile strength, MPa (ksi)	Elongation, %
Longitudinal	0.554 (0.218)	875 (127)	916 (133)	13.0
Minimum		827 (120)	896 (130)	10.0

between each roll. The initial thicknesses of the materials used were in the range of 0.554-0.671 cm (0.218-0.264 in.). One set of samples was cold rolled to a 5% reduction in thickness, while another was rolled to a 10% reduction in thickness. After rolling, both sets were annealed at 650 °C (1202 °F) for 4 h and furnace cooled. A third set of samples was cold rolled without annealing.

The second stage of processing involved 30% reductions in thickness with intermediate annealing. Annealing temperatures and times varied. Annealing times were 3, 4, and 5 h, at annealing temperatures of 600, 650, and 700 °C with furnace cooling. A second group was annealed at 650 °C for 4 h with air cooling.

The third stage of processing involved 10% reductions in thickness with intermediate annealing. In this stage, prior to annealing, samples were coated with CG44 thermal coatings to reduce the occurrence of oxidation. Annealing temperatures were 900, 1020, and 1200 °C for 1 h with air cooling. After annealing, coatings were removed by grit blasting and grinding, followed by further reductions in thickness. The fourth stage of the processing used similar temperature conditions. However, no coatings were used, and annealing time was increased to 2 h.

For the first four stages, both the standard and ELI Ti-6Al-4V alloys were treated with the same thermo-mechanical processes. However, during the fifth and final stages of testing, processing methods differed between the ELI and standard alloys.

The final stage of processing involved 10-15% reductions in thickness and intermediate annealing between each rolling. Standard alloy samples were annealed at 750 °C for 4 h and a separate set was annealed at 900 °C for 2 h. ELI samples were annealed at 800 °C and cooled in three different ways—air cooling, furnace cooling, and water quenching. After annealing, samples were machined to remove the oxidation layer.

Tensile testing was performed using tensile bars machined by using a Sodick AQ325L Electro Discharge Machining EDM. ASTM E8 Sub-size tensile bars were used during the first three stages of thermomechanical processes, and standard size ASTM E8 tensile bars were used for the final stage. Tensile specimens were prepared and tested in accordance with ASTM standard E8. The tensile samples were rectangular plate specimens, with 203.2-mm (8.0 in.) total length, 50.8-mm (2.0 in.) gauge length, 12.7-mm (0.5 in.) width, 57.15-mm (2.25 in.) length of reduced section, and 12.7-mm (0.5 in.) radius of fillet. The thickness of the samples was reduced to 6.35 mm (0.25 in.). The grips had 50.8-mm (2.0 in.) length, and 19.05-mm (0.75 in.) width. The ASTME sub-size tensile bars were also rectangular specimens with half of the standard size with the same proportions, and the thickness was 6.35 mm (0.25 in.). Tensile test were performed on an Instron 4505 test frame at a constant cross head speed of 1.27 mm/min (0.05 in./min).

Optical microscopy was performed in the final step for each thermomechanical process using an Olympus PME3 microscope. Microscopy samples were also taken mid-way during the final stage. This was performed to determine microstructural changes that occurred during the annealing process. Scanning electron microscopy (SEM) was performed on fractured samples using a Cambridge S-360 SEM unit. SEM micrographs were evaluated to determine possible mechanisms of fracture in the samples.

The crystallographic-preferred orientation distribution functions (ODF) were studied by determining (0002) pole figures for selected samples by x-ray diffraction using a Scintag 2-C-X1 Advanced Diffraction System and POPLA software (Ref 15).

3. Results and Discussion

From the standpoint of strength, the suitability of Ti-6Al-4V as a replacement for Ti-3Al-2.5V was never in question. However, other issues, most notably the formability and ductility of Ti-6Al-4V compared to Ti-3Al-2.5V became the main concern. From this study, it was evident that Ti-6Al-4V could be formed through cold working (through a limited design window), and could, therefore, be used as a tubing replacement. Design goals for the experiment included bringing the Ti-6Al-4V plate to the desired thickness of 0.081-0.094 cm (0.032-0.037 in.) and producing high tensile and yield strengths as compared to a Ti-3Al-2.5V while maintaining an adequate percent elongation.

Preliminary testing was performed to characterize the material properties of the as-received samples. The initial thickness of the as-received samples was 0.554-0.671 cm (0.218-0.264 in.). The thermomechanical schedule and test results are shown in Table 7. It is noted that the yield strengths of the as-received materials were lower than the numbers provided in the specifications and the percent elongations were much higher.

The effect of 5 and 10% cold work between intermittent annealing at 650 °C for 4 h and the effect of straight rolling (without annealing) are shown in Table 1. Preliminary testing indicated that Ti-6Al-4V was responsive to cold working as the tensile strength of the material increased after cold working. Tensile tests during the first stage of testing indicated that excessive cold work would not significantly increase the strength of Ti-6Al-4V since the strength increase of the 56.4% CW (without intermittent annealing) sample was not higher than that of the 5% or 10% CW samples. This was due to microcracking, which occurred from the excessive cold work.

Tensile testing of the ELI alloy generally showed that cold working would increase the tensile strength of the material. All the samples except for the 5% CW, annealed at 650 °C (1202 °F) for 4 h showed an increase in tensile strength in response to the cold rolling. This 5% rolled annealed sample could have shown a lower tensile strength due to microcracking, which was a common feature.

One interesting note was the high amount of cold work that the ELI alloy received without intermittent annealing. The ELI samples were rolled to an 88% reduction in thickness, more than 30% as compared to the standard samples. These samples also had higher tensile strengths compared to the lower reduction samples while maintaining a very good percent elongation value. However, the data were not consistent as shown by the results of the three samples which were rolled to 88% reduction in thickness.

A typical cold work calculation is shown in Table 8. It shows how the reduction in thickness due to milling operations was accounted for. Optical microscopy and SEM images of the fractured surfaces of the tensile bars are shown in Fig. 1 and 2. Microstructures of the as-received standard sample showed fine elongated grains. This indicated that the sample was subjected to hot rolling during the manufacturing process. Microstructures of the as-received ELI sample showed clustering of the beta phase (dark areas). Comparisons of the standard alloy,

Table 7 Stage 1 tensile testing results

Sample	Condition	Ultimate strength, MPa (ksi)	Yield strength, MPa (ksi)	Percent elongation	Fracture position(a)	Final thickness, cm (in.)	Total % CW
Ti-6Al-4V standard	As received	1063 (154.2)	788.1 (114.3)	32.8	Within	0.671 (0.264)	0.0
	5% CW, annealed at 650 °C (1202 °F) for 4 h	1314 (190.6)	1137 (164.9)	…	Out	0.089 (0.035)	32.0
	10% CW, annealed at 650 °C (1202 °F) for 4 h	1230 (178.4)	645.3 (93.6)	…	Out	0.089 (0.035)	27.7
	56.4% CW, no annealing	1215 (176.2)	668.8 (97.0)	7.8	Within	0.295 (0.116)	56.4
Ti-6Al-4V ELI	As received	945.3 (137.1)	783.9 (113.7)	28.8	Within	0.546 (0.215)	0.0
	5% CW, annealed at 650 °C (1202 °F) for 4 h	885.3 (128.4)	817.7 (118.6)	…	Out	0.0838 (0.033)	37.2
	10% CW, annealed at 650 °C (1202 °F) for 4 h	1236 (179.3)	777.7 (112.8)	9.6	Within	0.0838 (0.033)	23.3
	88% CW, no annealing	1725 (250.2)	1245 (180.6)	20.6	Within	0.0260 (0.066)	88.0
		1356 (196.7)	812.9 (117.9)	21.8	Within	0.0260 (0.066)	88.0
		1369 (198.5)	726.7 (105.4)	13.2	Within	0.0260 (0.066)	88.0

(a) Fracture position with respect to the marked gauge length. Within gauge length, the total percent elongation was calculated

Table 8 Calculation of cold working carried out to reduce thickness without including material loss due to milling; R defines a rolling step

Ti 6-Al-4V standard/commercial				
	5%		10%	
Stage	mm	in.	mm	in.
Initial	0.671	0.264	0.671	0.264
R1	0.605	0.238	0.632	0.249
After milling	0.521	0.205	0.460	0.181
R2	0.494	0.195	0.415	0.164
After milling	0.420	0.166	0.331	0.131
R3	0.381	0.150	0.288	0.114
After milling	0.240	0.0945	0.182	0.0715
R4	0.229	0.0900	0.165	0.0650
After milling	0.157	0.0620	0.127	0.0500
R5	0.0864	0.0340	0.0762	0.0300
Total milling	0.370	0.146	0.401	0.158
% CW total		32.0		28.8

R = Roll; R1 = first rolling reduction in thickness

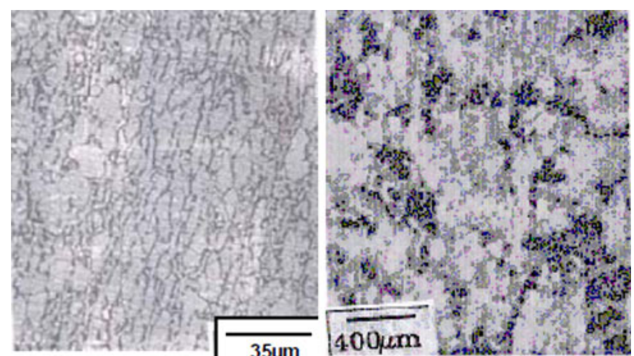

Fig. 1 Optical microstructures of Ti-6Al-4V for various conditions in transverse direction: (a) as-received standard; (b) as-received ELI

10% rolled and annealed, and 56.4% rolled with no annealing, microstructures show similar elongated grains. Since these microstructures were taken at the final stage of rolling, it is not clear whether recrystallization or partial recrystallization occurred for the rolled/annealed samples at these intermediate steps. SEM images of the as-received standard sample in Fig. 2(a) showed equiaxed dimples which imply a ductile fracture (32.8% elongation). In other conditions, for example Fig. 2(b), there were mixed mode fractures where equiaxed dimples were side by side to cleaved areas (Ref 16).

The second stage of thermomechanical processing and testing was performed to further refine the cold working and annealing design window. In this stage of testing, cold work was increased to 30% reduction in thickness in between annealing for all the samples. Elongation results could not be obtained for most broken tensile samples since these samples broke outside the gauge length. The second stage of testing was used to further develop an optimized thermomechanical schedule for Ti-6Al-4V. The thermo-mechanical process and the data for the tensile test of the sample after the final reduction in thicknesses are shown in Table 9. A graph of data from Table 9 is shown in Fig. 3. It was clear during the second phase that there was a lower temperature limit for the annealing of Ti-6Al-4V. All the standard samples annealed at 600 °C fractured during the subsequent cold rolling process. The phase diagram of Ti-6Al-4V does not show any brittle phases at this temperature. These fractures indicated that annealing at 600 °C did little to promote recovery and reduce internal stresses present in the alloy.

Ultimate strength properties for the cold-worked and annealed samples were improved. Air-cooled samples exhibited slightly higher tensile strengths compared to furnace-cooled samples due to the faster cooling rate (Ref 9, 17). There was a large amount of inconsistency within the tensile data. For example, ultimate strength values for the two standard samples annealed at 650 °C (1202 °F) showed one sample with a tensile strength nearly three times greater than the other sample (with the same heat treatment and cold work). This inconsistency can

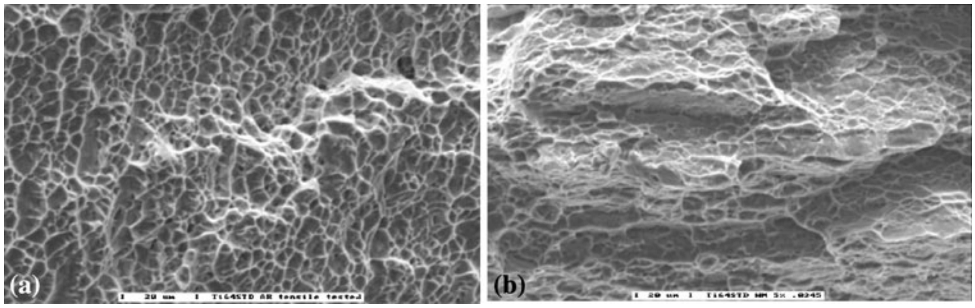

Fig. 2 SEM images of standard Ti-6Al-4V for fractured tensile bars: (a) as received; (b) 5% reduction with intermediate annealing at 650 °C (1202 °F) for 4 h

Table 9 Stage 2 tensile testing results, samples rolled to 30% reduction in thickness between annealing times and temperatures indicated above

Sample	Annealing condition		Ultimate strength, MPa (ksi)	Yield strength, MPa (ksi)	Percent elongation	Fracture position(a)	Final thickness, cm (in.)	Total % CW
	Temp., °C	Time, h						
Ti-6Al-4V standard	600	3	X	X	X	X	X	X
	650	3	1290 (187.1)	828.0 (120.1)	…	Out	(0.079) 0.031	67.9
	650	3	436 (63.2)	367.0 (53.2)	…	Out	0.079) 0.031	67.9
	700	3	1259 (182.6)	1246 (180.7)	…	Out	0.089 (0.035)	66.3
	700	3	848.0 (123.0)	684.0 (99.2)	…	Out	0.089 (0.035)	61.3
	600	4	X	X	X	X	X	X
	650	4	1131 (164.0)	955 (138.5)	…	Out	0.089 (0.035)	66.3
	650	4	1415 (205.2)	1398.0 (202.8)	…	Out	0.089 (0.035)	66.3
	650(b)	4	1393 (202.0)	816.0 (118.4)	…	Out	0.084 (0.033)	65.2
	650(b)	4	1384 (200.7)	1264.0 (183.3)	…	Out	0.084 (0.033)	65.2
	700	4	1289 (187.0)	799.0 (115.9)	…	Out	0.086 (0.034)	58.8
	600	5	X	X	X	X	X	X
	650	5	XX	XX	XX	XX	XX	XX
	700	5	1290 (187.1)	828.0 (120.1)	…	Out	0.081 (0.032)	61.1
	As received		1063 (154.2)	788.1 (114.3)	32.8	Within	0.671 (0.264)	0.0
Ti-6Al-4V ELI	600	3	1266 (183.6)	1247 (180.8)	…	Out	0.086 (0.034)	61.3
	600	3	1265 (183.5)	756.4 (109.7)	6.8	Within	0.086 (0.034)	61.3
	650	3	1328 (192.6)	732.2 (106.2)	…	Out	0.086 (0.034)	59.8
	700	3	1183 (171.6)	1176 (170.5)	…	Out	0.091 (0.036)	61.3
	700	3	1221 (177.1)	680.5 (98.7)	…	Out	0.091 (0.036)	61.3
	600	4	1245 (180.5)	1227 (177.9)	…	Out	0.091 (0.036)	62.1
	650(b)	4	1218 (176.7)	1198 (173.8)	…	Out	0.089 (0.035)	60.7
	650(b)	4	1264 (183.3)	838.4 (121.6)	…	Out	0.091 (0.036)	69.8
	700	4	1214 (176.1)	762.6 (110.6)	…	Out	0.091 (0.036)	64.0
	600	5	1249.7 (181.2)	849.4 (123.2)	11.6	Within	0.091 (0.036)	66.1
	600	5	1257 (182.3)	1243 (180.3)	…	Out	0.091 (0.036)	66.1
	650	5	1299 (188.4)	841.2 (122.0)	…	Out	0.089 (0.035)	69.3
	700	5	1160 (168.2)	641.2 (93.0)	…	Out	0.091 (0.036)	67.4
	700	5	1172 (170.0)	1157 (167.8)	…	Out	0.091 (0.036)	67.4
	As received		945.3 (137.1)	783.9 (113.7)	28.8	Within	0.546 (0.215)	0.0

All samples except for one were furnace cooled. X: Denotes samples fractured during rolling. XX: Denotes samples bent and warped during rolling (a) Fracture position with respect to the marked gauge length. Within gauge length, then total percent elongation was calculated. (b) Denotes air-cooled sample

be attributed to microcracking which was caused when the material was subjected to a large amount of cold work (30% reduction in thickness) possibly without intermittent recovery or softening. Although samples were annealed, annealing temperatures and times may have been insufficient to cause recovery and recrystallization.

ELI tensile testing showed increases in ultimate strengths from the as-received ELI sample, as all the samples showed increase in strength except for one of the samples annealed at 600 °C for 5 h. The ELI sample that failed below the tensile strength of the as-received material could have failed due to microcracking, much like in the standard grade alloy. All except for the two rolled and heat-treated ELI samples (600 °C for 3 and 5 h) broke outside of the gauge length.

Optical microscopy and SEM images are shown in Fig. 4 and 5. Optical microscopy showed much of the same fine

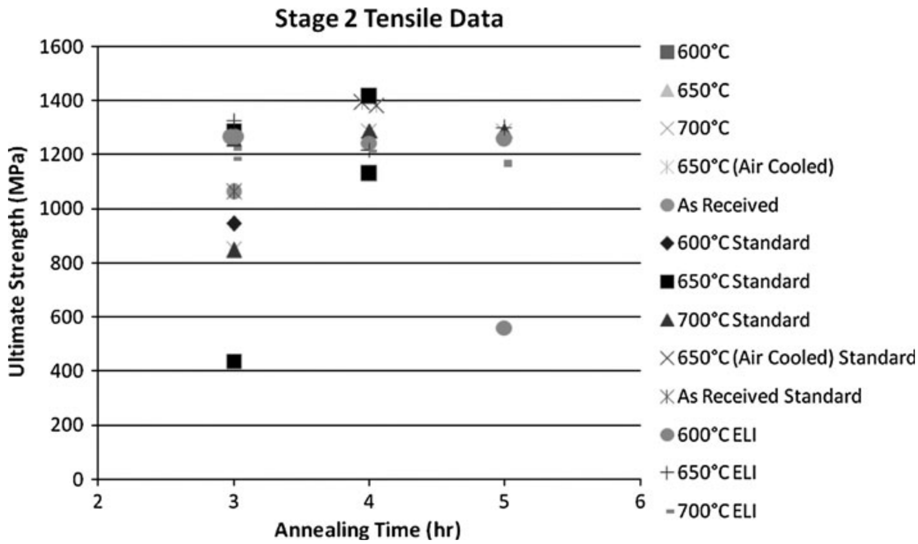

Fig. 3 Stage 2 tensile data for Ti-6Al-4V alloy

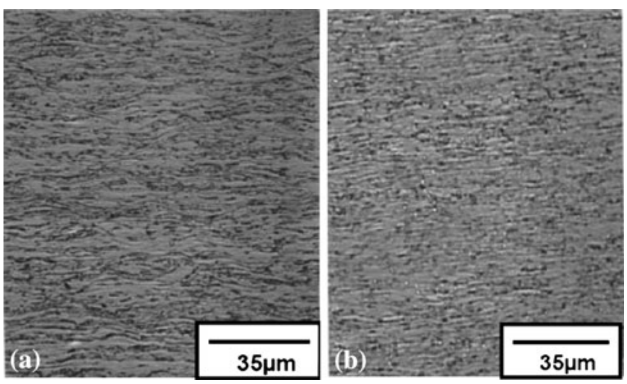

Fig. 4 Second stage optical microstructures of standard Ti-6Al-4V in the longitudinal direction with a 30% reduction with intermediate annealing at (a) 600 °C (1112 °F) for 3 h; (b) 650 °C (1202 °F) for 4 h

elongated grains that were present in preliminary testing. All images in Fig. 4, 30% reduction with intermediate annealing at 600 °C for 3 h, 650 °C (1202 °F) for 4 h, and 650 °C (1202 °F) for 5 h, showed elongated grains. Similar to the first stage heat-treated samples, these microstructures were taken only in the rolled state after the final reduction in thickness condition. SEM images in Fig. 5 revealed mixed mode fracture areas. Microcracks were probably the source of the sample fracture outside the gauge length as well as the variance in tensile data. The stress-strain diagrams also showed striation lines in all the tests.

Following the second stage of testing the Stanat cold roller used for the experiments fractured. This failure could be attributed to the extensive cold work (88% reduction in thickness) without intermittent annealing performed during preliminary testing. It was, therefore, recommended that small amounts of cold work with intermediate annealing be performed on Ti-6Al-4V.

The third stage of testing involved the use of coatings to reduce oxide buildup on samples after annealing. The thermo-mechanical processing and tensile testing of the final rolled samples are shown in Table 10. Cold work in this stage was decreased to 10% reduction in thickness between annealing, and the annealing temperatures were raised to 900, 1020, and 1200 °C. In addition, the samples were tensile tested in the stress-relieved condition (400 °C for 1 h) rather than in the final rolled condition as in previous stages. Optical microscopy images are shown in Fig. 6. This stage also utilized a new rolling mill located at Caltech, a Stanat CX-100, a less powerful model as compared to the FX-200 used in previous phases. During the third stage of testing, thermomechanical processing was modified in an attempt to reduce oxide buildup during the annealing process. CG-44 coating was employed to improve material resistance to oxidation. However, it was not easily removed, neither with grit blasting nor machining. Although coatings significantly reduced oxidation and subsequent material loss due to machining, an easier way of removing the coating should be devised since the overall material recovered would not make up for the time spent removing the coating. In an actual implementation of these processes, a vacuum furnace should be used.

Tensile tests resulted in ultimate strengths for two conditions (both standard and ELI) that were lower than the as-received sample. This was probably again due to the initiation of microcracks and the new rolling mill utilized during testing, which was not sufficiently powerful to plastically deform the Ti-6Al-4V samples to the desired thicknesses. Both ELI and standard samples annealed at 1200 °C fractured during rolling as shown in Table 10.

The 900 °C-annealed (Fig. 6a, d) microstructures showed large equiaxed grains, which indicate recrystallization since the grains were not elongated (as opposed to the as-received, stages 1 and 2 microstructures). Microstructures explained the fractures of the samples annealed at 1200 °C. The phase diagram for Ti-6Al-4V indicates that 1200 °C exceeds the beta transus temperature of the material (Ref 9). Consequently, the microstructure of these annealed samples reveals an acicular basketweave type of grain structure (Fig. 6b, e), strongly contributing to its brittle nature. Samples annealed at 1020 °C (Fig. 6c, f) also exhibited this acicular structure with

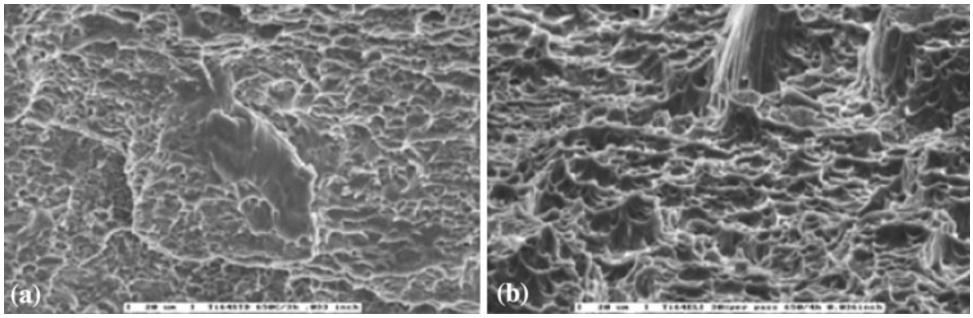

Fig. 5 SEM microstructures of standard Ti-6Al-4V with a 30% reduction with intermediate annealing at (a) 650 °C (1202 °F) for 3 h; (b) 650 °C (1202 °F) for 4 h

Table 10 Stage 3 tensile testing results, samples rolled to 10% reduction in thickness

Sample	Annealing condition		Ultimate strength, MPa (ksi)	Yield strength, MPa (ksi)	Percent elongation	Fracture position(a)	Final thickness, cm (in.)	Total % CW
	Temp., °C	Time, h						
Ti-6Al-4V standard	900	1	1055 (153.0)	747 (108.3)	13.1	Within	0.528 (0.2079)	19.0
			988 (143.3)	685 (99.4)	…	Out	0.528 (0.2079)	19.0
	1020	1	987 (143.2)	568 (82.4)	7(b)	Within	0.528 (0.2079)	19.0
			945 (137.1)	765 (111.0)	…	Out	0.528 (0.2079)	19.0
	1200	1	X	X	X	X	0.538 (0.2118)	15.0
			X	X	X	X	0.538 (0.2118)	15.0
	As received		1063 (154.2)	788.1 (114.3)	32.8	Within	0.671 (0.264)	0.0
Ti-6Al-4V ELI	900	1	946.7 (137.3)	616.6 (89.4)	13.3	Within	0.441 (0.1735)	18
			961.1 (139.4)	761.2 (110.4)	…	Out	0.441 (0.1735)	18.0
	1020	1	X	X	X	X	0.437 (0.172)	18.0
			XX	XX	XX	XX	0.437 (0.172)	18.0
	1200	1	X	X	X	X	0.450 (0.1770)	15.0
			X	X	X	X	0.450 (0.1770)	15.0
	As received		945.3 (137.1)	783.9 (113.7)	28.8	Within	0.546 (0.215)	0.0

Samples tensile tested in stress-relieved state (400 °C for 1 h) and thermal barrier coating used for each sample. Samples tested at a cross-head speed of 0.064 cm/min (0.025 in./min) vs. 0.127 cm/min (0.05 in./min) as with previous samples. X: Denotes fracture during rolling. XX: Not tested
(a) Fracture position with respect to the marked gauge length. Within gauge length, then total percent elongation was calculated. (b) Extensiometer broke during testing

enlarged grains and exhibited a similar reduction in ductility. Interestingly, the 1020 °C standard-annealed sample also showed lower tensile strength values than the 900 °C (1652 °F)-annealed samples. This drop in tensile strength was probably due to grain growth which occurred due to the higher annealing temperature.

Microstructure images and tensile tests strongly advocate 900 °C (1652 °F) for 1 h as a proper annealing condition for the Ti-6Al-4V alloy. The other two conditions, however, were unsuitable for rolling due to the brittleness of the beta phase as evident from tensile testing and microstructures. The fourth stage of thermomechanical processing involved further refinement of the cold-working-annealing design window. Tensile test results for the fourth stage of testing are shown in Table 11. Optical microscopy images are shown in Fig. 7.

The fourth stage tested Ti-6Al-4V alloy under similar conditions to stage 3, but with one more hour of annealing time to stimulate softening by partial recrystallization. In addition, stage 4 testing used a more powerful LOMA rolling mill (15 hp, 100 A motor) that could easily deform the titanium samples down to the desired final thickness. Consequently, 900 °C (1652 °F)-annealed samples showed an increase in strength as compared to the stage 3 samples and the as-received sample with an average ultimate strength ~1240 MPa (~180 ksi). It should be noted that in the first two stages, samples were tensile tested in the final rolled condition. In this stage and the previous stage, the samples were tested in the stress-relieved condition at 400 °C for 1 h. Stage 4 tensile testing also confirmed the brittleness associated with samples annealed above the beta transus temperature. Standard samples annealed at 1020 °C (1868 °F) exhibited much lower tensile strengths (~870 MPa, ~127 ksi), and similar to those of stage 3 testing, samples annealed at 1200 °C (2192 °F) fractured during the rolling process. One interesting comparison is between the ELI and standard Ti-6Al-4V samples at the 900 °C annealing temperature. In this situation, the ELI alloy showed much lower ultimate strength values than those of the standard alloy.

Optical microscopy revealed grain growth for each of the samples, most notably Fig. 7(c) and (d), the samples heated above the beta transus temperature. This was expected since the annealing time of each temperature was increased by 1 h. At these annealing times, the acicular grains of the 2 h 1020 and 1200 °C annealed samples were significantly larger than those annealed for 1 h in stage 3.

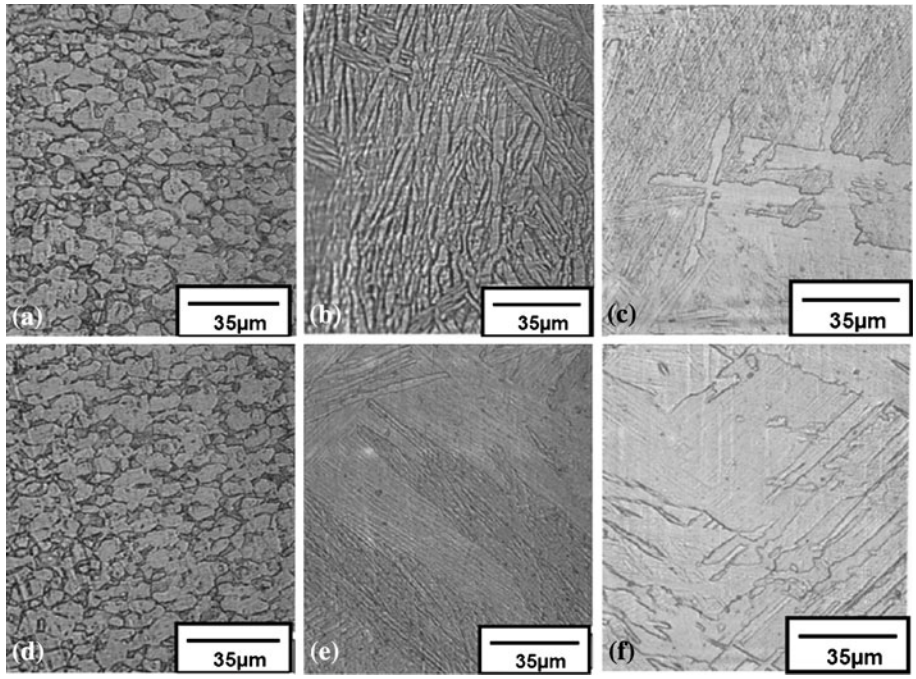

Fig. 6 Third stage optical microstructures of standard Ti-6Al-4V with a 10% reduction with intermediate annealing at (a) 900 °C (1652 °F) for 1 h longitudinal; (b) 1020 °C (1868 °F) for 1 h longitudinal; (c) 1200 °C (2192 °F) for 1 h longitudinal; (d) 900 °C (1652 °F) for 1 h transverse; (e) 1020 °C (1868 °F) for 1 h transverse; (f) 1200 °C (2192 °F) for 1 h transverse

Table 11 Stage 4 tensile testing results, samples rolled at 10% reduction in thickness

Sample	Annealing condition		Ultimate strength, MPa (ksi)	Yield strength, MPa (ksi)	Percent elongation	Fracture position(a)	Final thickness, cm (in.)	Total % CW
	Temp., °C	Time, h						
Ti-6Al-4V standard	900	2	1241 (180.0)	661 (95.9)	6	Within	0.15 (0.059)	33
			1233 (178.8)	864 (125.3)	3	Within	0.15 (0.059)	33
	1020	2	842 (122.1)	…	…	Out	0.152 (0.06)	32
			909 (131.8)	…	…	Out	0.152 (0.06)	32
	1200	2	X	X	X	X	0.183 (0.072)	20
			X	X	X	X	0.183 (0.072)	20
	As received		1063 (154.2)	788.1 (114.3)	32.8	Within	0.671 (0.264)	0.0
Ti-6Al-4V ELI	900	2	1183 (171.7)	1091 (158.4)	…	Out	0.147 (0.058)	37
			1166 (169.2)	1162 (168.6)	…	Out	0.147 (0.058)	37
	1020	2	400 (58)	…	…	Out	0.157 (0.062)	33
			505 (73.3)	…	…	Out	0.157 (0.062)	33
	1200	2	X	X	X	X	0.193 (0.076)	18
			X	X	X	X	0.193 (0.076)	18
	As received		945.3 (137.1)	783.9 (113.7)	28.8	Within	0.546 (0.215)	0.0

Samples tensile tested in stress relieved state at 400 °C for 1 h. Samples tested at a cross-head speed of 0.064 cm/min (0.025 in./min)
(a) Fracture position with respect to the marked gauge length. Within gauge length, then total percent elongation was calculated

The fifth stage tested thermomechanical processing conditions deemed optimal based on the first four stages. Tensile test results for the fifth stage of testing are shown in Table 12 and 13.

The standard and ELI samples had different schedules. In Table 12, the standard sample was rolled at 10-15% reduction in thickness between annealing at 900 °C for 2 h and another set at 750 °C for 4 h. The starting (as received) material for the standard alloy was changed into a thinner plate to reduce the probability of having a large distribution of initial cracks in the material (Ref 16, 18). The starting standard Ti-6Al-4V material was changed to a thinner plate of 0.254 cm (0.1 in.). This was less than half the thickness of the material used in the first four stages. Optical microscopy and SEM images are shown in Fig. 8-10. (0002) pole figures are shown in Fig. 11.

Table 13 shows tensile test results for the ELI samples. The thickness of the ELI material was not changed because a 0.254 cm (0.1 in.) thickness plates were not available. ELI samples were cold worked to a 10-15% reduction in thickness with intermediate annealing at 800 °C for 2 h. The samples were then divided into three groups which were cooled by air cooling, water quenching, and furnace cooling to determine

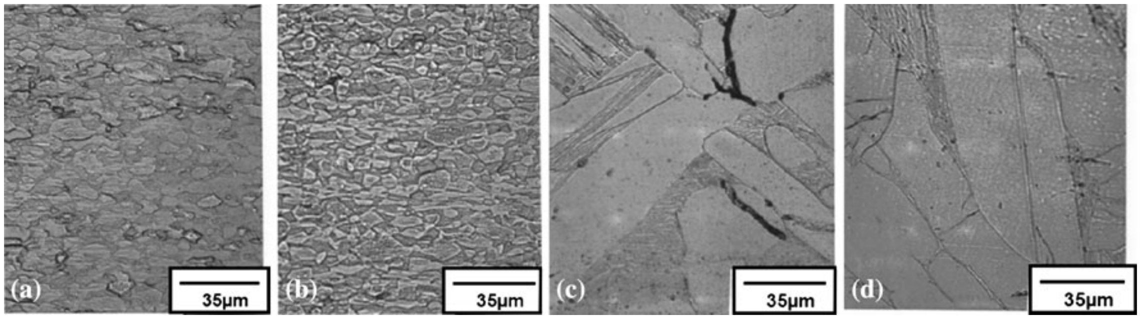

Fig. 7 Fourth stage optical microstructures of standard Ti-6Al-4V with a 10% reduction and intermediate annealing at (a) 900 °C (1652 °F) for 2 h longitudinal; (b) 900 °C (1652 °F) for 2 h transverse; (c) 1200 °C (2192 °F) for 2 h longitudinal; (d) 1200 °C (2192 °F) for 2 h transverse

Table 12 Stage 5 tensile testing of standard Ti-6Al-4V results, samples rolled from an initial thickness of 0.254 cm (0.1 in.) to 10-15% reduction in thickness with an intermediate anneal

Sample condition	Ultimate strength, MPa (ksi)	Yield strength, MPa (ksi)	Percent elongation	Fracture position(a)	Final thickness, cm (in.)	Total % CW
As received	1042 (151.1)	993 (144.0)	19.1	Within	0.254 (0.1)	0
	1041 (150.9)	994 (144.1)	10	Out	0.254 (0.1)	0
	1042 (151.1)	963 (139.6)	19.8	Within	0.254 (0.1)	0
Annealed 900 °C (1652 °F) for 2 h	888 (128.8)	203 (29.4)	…	Out	0.081 (0.032)	52
	800 (116.0)	…	…	Out	0.086 (0.034)	52
	799 (115.9)	798 (115.7)	…	Out	0.086 (0.034)	52
	823 (119.3)	676 (98.0)	…	Out	0.091 (0.036)	52
	780 (113.1)	…	…	Out	0.084 (0.033)	52
	794 (115.1)	…	…	Out	0.081 (0.032)	52
	897 (130.1)	889 (128.9)	…	Out	0.084 (0.033)	52
Annealed 750 °C (1382 °F) for 4 h	1017 (147.5)	956 (138.6)	10.8	Within	0.097 (0.038)	62
	1025 (148.6)	960 (139.2)	11.8	Out	0.097 (0.038)	62
	1044 (151.4)	958 (138.9)	5.5	Out	0.094 (0.037)	62
	1007 (146.0)	943 (136.7)	10.3	Within	0.097 (0.038)	62
	1038 (150.5)	956 (138.6)	5.8	Out	0.097 (0.038)	62
	1059 (153.6)	1002 (145.3)	7.3	Within	0.094 (0.037)	62
	1100 (159.5)	894 (129.6)	10.8	Within	0.091 (0.036)	62
	1074 (155.7)	978 (141.8)	10.8	Within	0.094 (0.037)	62
	1048 (152.0)	153 (22.2)	11.2	Within	0.094 (0.037)	62
	1100 (159.5)	1004 (145.6)	6	Out	0.094 (0.037)	62
	1072 (155.4)	985 (142.8)	11.2	Within	0.094 (0.037)	62

Samples tensile tested in annealed state with full sized ASTM E8 tensile bars. As-received sample was not rolled or annealed. As-received sample was a thinner plate (0.254 cm) as compared to the material (0.67 cm) that was used in all previous experiments
(a) Denotes fracture position (within or outside of gauge length)

responses to cooling rate. During the final two anneals before samples were brought to the final thickness, annealing time was reduced to 1 h to reduce oxide buildup.

The final stage of testing involved testing standard samples within the derived design window of thermomechanical parameters, 10-15% cold work with annealing conditions of 900 °C (1652 °F) for 2 h and 750 °C (1382 °F) for 4 h. Annealing at 750 °C yielded tensile strength values comparable to the as-received samples. Samples annealed at 900 °C exhibited much lower strength values than that of the as-received alloy annealed at 750 °C, and as-received samples. It should be noted that at this stage the samples were tensile tested in the annealed condition as compared to the as-rolled condition (stages 1 and 2) and the stress relieved conditions (stages 3 and 4).

ELI samples experienced slight changes in ultimate strength from the as-received material with an average increase of ~50 MPa for air-cooled samples and decreases of ~40 MPa and ~30 MPa for the furnace-cooled and water-quenched sample, respectively. Surprisingly, the ELI alloys that were water quenched did not show gains in tensile strength, which is a contradiction to what normally happens with an increased cooling rate (Ref 17). This may be attributed to the omega phase forming during water quenching. If a titanium alloy is worked or heated above 1200 °F without being furnace cooled through the 1200-1000 °F it promotes the formation of omega causing the alloy to harden and embrittle (Ref 19). The air-cooled sample showed a slight increase in tensile strength. While there were no significant gains in tensile strength, each sample condition showed a large decrease in ductility. This loss in ductility also occurred in the standard grade alloy samples.

Optical microscopy of the new as-received 0.254 cm (0.1 in.) thick standard samples in Fig. 8 showed fine, equiaxed grains. When Fig. 8 is compared with Fig. 1(a), it is clear that

Table 13 Stage 5 tensile testing results of ELI Ti-6Al-4V, samples rolled from an initial thickness of 0.254 cm (0.1 in.) to 10-15% reduction in thickness with an intermediate anneal

Sample condition	Ultimate strength, MPa (ksi)	Yield strength, MPa (ksi)	Percent elongation	Fracture position(a)	Final thickness, cm (in.)	Total % CW
As received	945.3 (137.1)	783.9 (113.7)	28.8	Within	0.546 (0.215)	0.0
Annealed at 800 °C air cooled	1117 (162.0)	452 (65.5)	…	Out	0.052 (0.020)	59.5
	1034 (149.9)	1034 (149.9)	…	Out	0.052 (0.020)	59.5
	937 (135.8)	852 (123.6)	12.3	Within	0.052 (0.020)	59.5
	970 (140.6)	883 (128.0)	12	Within	0.052 (0.020)	59.5
	981 (142.3)	891 (129.2)	10	Within	0.052 (0.020)	59.5
	979 (141.9)	860 (124.7)	9.25	Within	0.052 (0.020)	59.5
	930 (134.8)	837 (121.4)	12.25	Within	0.052 (0.020)	59.5
	852 (123.5)	759 (110.1)	…	Out	0.052 (0.020)	59.5
Annealed at 800 °C furnace cooled	997 (144.6)	706 (102.4)	11.3	Within	0.049 (0.019)	62
	986 (143.0)	950 (137.8)	10.85	Within	0.049 (0.019)	62
	951 (137.9)	936 (135.7)	…	Out	0.049 (0.019)	62
	1015 (147.2)	954 (138.3)	10.35	Within	0.049 (0.019)	62
	983 (142.6)	944 (136.9)	…	Out	0.049 (0.019)	62
	1014 (147.0)	973 (141.1)	9.25	Within	0.049 (0.019)	62
Annealed at 800 °C water quenched	1008 (146.1)	379 (55.0)	…	Out	0.059 (0.023)	57.8
	997 (144.5)	975 (141.4)	…	Out	0.059 (0.023)	57.8
	951 (137.9)	912 (132.3)	…	Out	0.059 (0.023)	57.8
	1003 (145.5)	946 (137.2)	…	Out	0.059 (0.023)	57.8
	935 (135.6)	848 (123.0)	…	Out	0.059 (0.023)	57.8
	960 (139.2)	884 (128.2)	…	Out	0.059 (0.023)	57.8
	1038 (150.5)	981 (142.2)	…	Out	0.059 (0.023)	57.8
	976 (141.5)	946 (137.1)	…	Out	0.059 (0.023)	57.8
	1007 (146.0)	934 (135.5)	…	Out	0.059 (0.023)	57.8

Samples tensile tested in annealed state with full sized ASTM E8 tensile bars. As received sample was not rolled or annealed. As received sample was the same ELI plate used throughout the experiment
(a) Denotes fracture position (within or outside of gauge length)

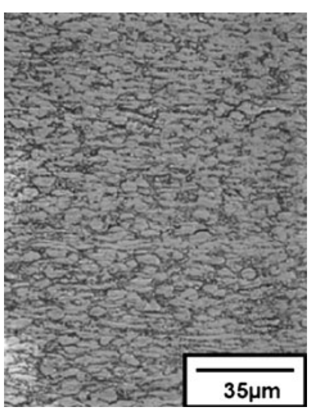

Fig. 8 Fifth stage optical microstructures of Ti-6Al-4V as-received sample 0.254-cm (0.1 in.)-thick, longitudinal section

the initial as-received sample (0.254 cm) was exposed to more extensive hot rolling as revealed by its elongated grains. Figure 9(a)-(c), microstructures of the 900 °C (1652 °F) annealed for 2 h samples, showed large equiaxed grains. This was an indication of partial or full recrystallization and subsequent grain growth. Grains of this condition were much larger ($\sim 2-3x$) compared to those of the as-received samples. The lower tensile strengths of the 900 °C (1652 °F) annealed for the 2 h samples can be attributed to this grain growth, since larger grains degrade strength due to less grain boundaries to stop dislocation motion (Ref 17). The microstructure of the 750 °C (1382 °F) for 4-h-annealed samples, Fig. 9(d)-(f) showed finer grains than the 900 °C (1652 °F) samples. However, the microstructure for the final sample showed elongated grains, similar to those seen in rolled samples. As in previous stages, it would appear that 750 °C (1382 °F) for 4 h may not be a sufficient cold rolling-annealing condition to promote recrystallization. One interesting comparison is the microstructure of the 900 °C (1652 °F)-annealed sample before and after annealing(9A and B) and the microstructure of the 750 °C (1382 °F)-annealed sample before and after annealing (Fig. 9d, e). Figure 9(a) shows a microstructure with somewhat equiaxed grains similar to Fig. 9(b). In contrast, Fig. 9(d) and (e) display somewhat elongated grains which may imply partial or incomplete recrystallization. Figure 9(a) is a sample after completing 10% cold work before annealing.

Microstructures for the ELI alloy were more similar to the 750 °C annealed for 2 h samples than to the 900 °C annealed for 1 h sample of the standard alloy. Here, the microstructure looks somewhat equiaxed, but elongated in comparison to the 900 °C-annealed samples. The furnace-cooled sample (Fig. 9i) showed equiaxed grains which indicate partial or full recrystallization.

SEM images for the as-received and 750 °C (1382 °F)-annealed samples showed ductile fracture with equiaxed dimples.

Figure 11 shows (0002) recalculated pole figures for various heat treatment conditions above. The results showed a texture severity of 4.9× random for the as-received sample with

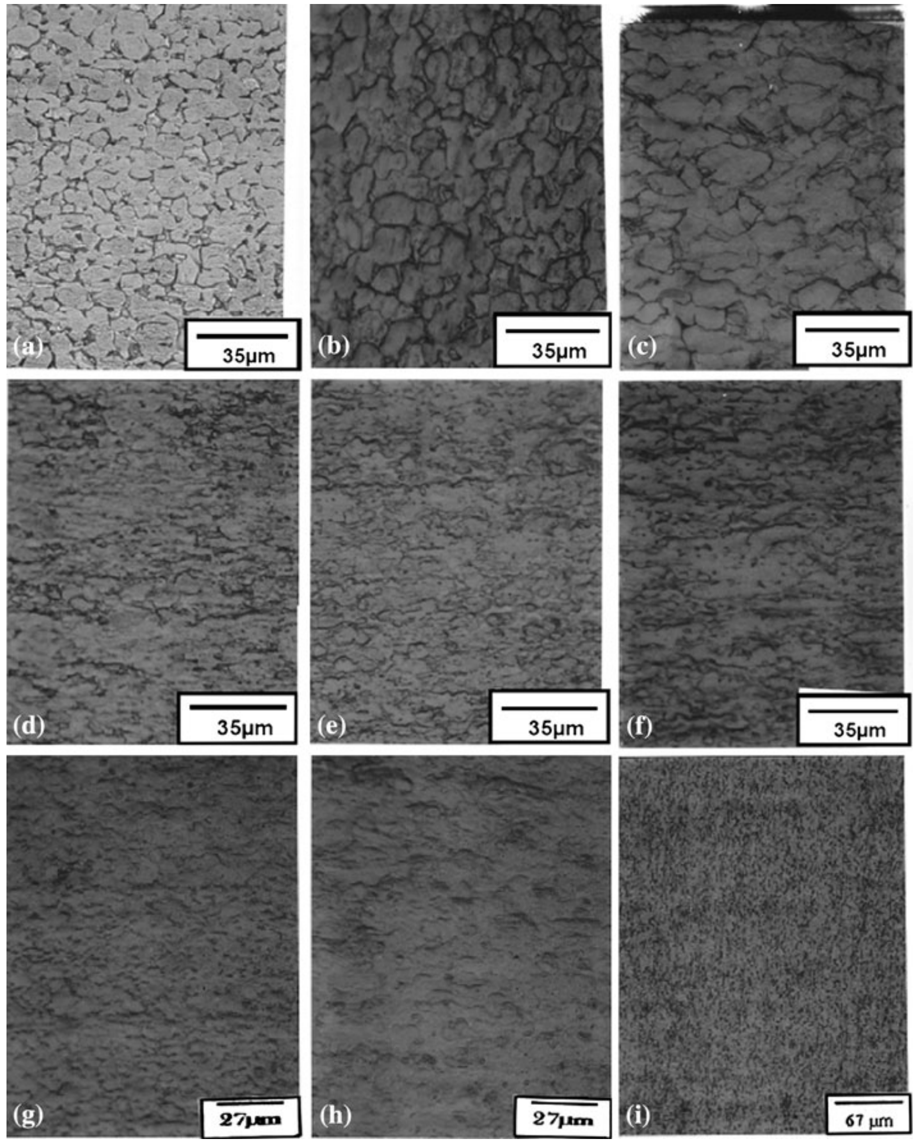

Fig. 9 Fifth stage optical microstructures of Ti-6Al-4V for all conditions in the longitudinal direction with a 10% reduction in thickness and intermediate annealing at (a) 900 °C (1652 °F) for 2 h midway before annealing (standard); (b) 900 °C (1652 °F) for 2 h midway after annealing (standard); (c) 900 °C (1652 °F) for 2 h after annealing final (standard); (d) 750 °C (1382 °F) for 4 h midway before annealing (standard); (e) 750 °C (1382 °F) for 4 h midway after annealing (standard); (f) 750 °C (1382 °F) for 4 h after at final thickness (standard); (g) 800 °C (1382 °F) for 2 h, water quenched at final thickness (ELI); (h) 800 °C (1382 °F) for 2 h, air cooled at final thickness (ELI); (i) 800 °C (1382 °F) for 2 h, furnace cooled at final thickness (ELI)

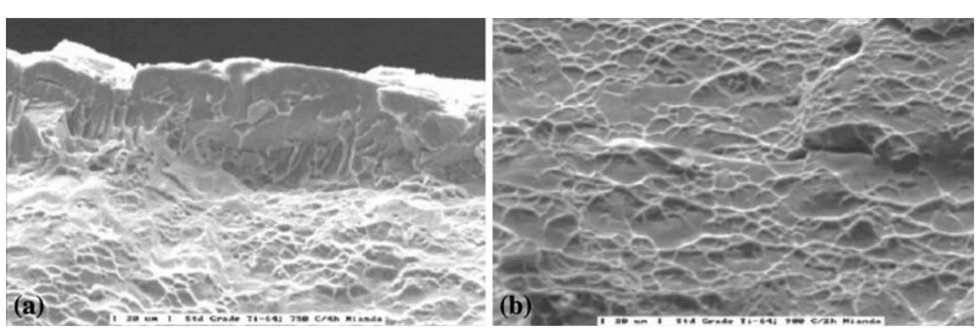

Fig. 10 SEM images of standard Ti-6Al-4V for all conditions at various magnifications: (a) 10% reduction, intermediate annealing at 750 °C (1382 °F) for 4 h after annealing final; (b) 10% reduction, intermediate annealing at 900 °C (1652 °F) for 2 h after annealing final

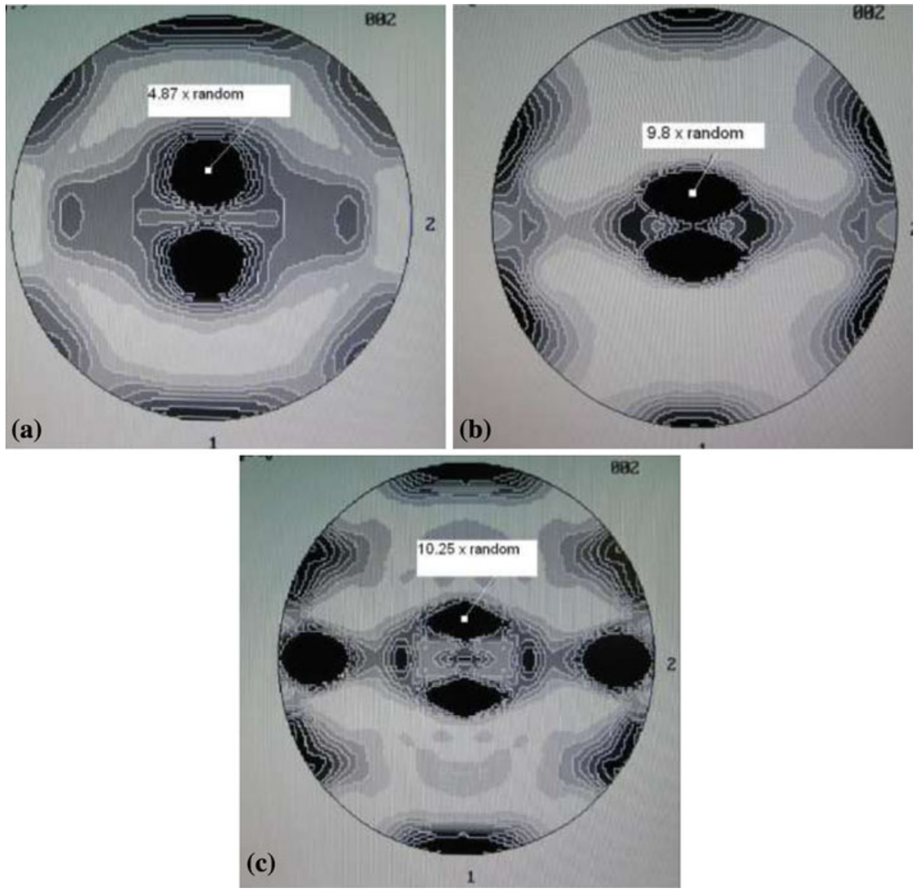

Fig. 11 Recalculated (0002) pole figures standard alloy at specific condition: (a) as received; (b) intermittent annealing at 750 °C (1382 °F) for 4 h; (c) intermittent annealing at 900 °C (1382 °F) for 2 h

subsequent texture sharpening in the 10% cold worked with 700 and 900 °C annealing with values of 9.8× random and 10.2× random, respectively. This level of texture severity is expected because of the excessive cold work received by both samples during processing stages. The ELI samples showed similar results with an increase in texture severity between the as-received sample (4.3× random) and the cold-worked samples which were furnace cooled (7× random), air cooled (5.1× random) and water quenched (8.2× random).

Tensile tests of the 750 °C (1382 °F) for 4-h-annealed standard alloy samples provided the most consistent data, as most of the samples broke within the gauge length. These samples also maintained low scatter in tensile strengths with respect to the as-received samples. This consistency was probably due to the annealing condition, which, although it might not have resulted in full recrystallization, did act as a stress relieving anneal for the material. The 900 °C (1652 °F) sample annealed for 2 h showed lower tensile strengths than both the as-received and 750 °C (1382 °F) for 4 h annealed samples. This loss in strength could be attributed to excessive grain growth due to the higher temperature of annealing. Had samples been annealed for a shorter amount of time (30 min-1 h) strength values probably would have been higher. Evidence of this is seen in stages 3 and 4 where samples annealed at 900 °C (1382 °F) for 1 h showed very high tensile strengths.

The scatter in the early stages in all tensile data can be related to the springback effect of Ti-6Al-4V samples and the subsequent formation of microcracks. Also the process of non-uniform oxide removal could have contributed to this problem.

4. Conclusions

The following were concluded from this study:

- It is possible to cold roll Ti-6Al-4V and anneal it to achieve desired mechanical properties and thickness for hydraulic tubing.
- When cold rolling, the reduction in thickness should not exceed 10-15% before annealing the sample.
- Ti-6Al-4V should be annealed between 650 °C (1202 °F) and 900 °C (1652 °F), or below the beta transus temperature for optimal tubing mechanical properties, since temperatures below 650 °C for the standard—and above 1000 °C for both—cause fracture. It should be also noted that at above 900 °C, excessive grain growth occurs.
- Samples annealed at the lower end of the recommended range should be annealed for longer periods of time (4-5 h) to ensure complete recrystallization.
- Samples annealed at the upper end of the recommended range should be annealed for shorter periods of time (30 min) to prevent excessive grain growth.
- Annealing temperature of 750 °C produced high strength samples with moderate ductility.

- Air cooling of samples provided slightly improved strength, while water quenching of the sample may have promoted the omega phase.
- The final sample as in the case of the initial sample in Ti-6Al-4V should be annealed to prevent microcracking and variation in test results.
- The original starting thickness of the samples, 0.55-0.67 cm (0.215-0.264 in.) used in this study is probably too thick as a starting material to reach a thickness of 0.081-0.094 cm (0.032-0.037 in.). A starting thickness of 0.254 cm (0.1 in.) is probably sufficient to induce a window of cold work stress relief (CWSR) and maximize the properties without inducing micro-cracks.
- The cooling rate effect on the mechanical properties of thermomechanically processed Ti-6Al-4V should be further investigated.

References

1. J.F. Zugschwert, *Tiltrotor and Advanced Rotorcraft Technology in the National Airspace System (TARTNAS)*, 01 Mar 2001, FAA RE&D Committee Vertical Flight Subcommittee, http://www.faa.gov/about/office_org/headquarters_offices/ato/service_units/nextgen/research_planning/redac/reports/media/pdf/TARTNAS_Final_Report.pdf
2. V-22 Osprey, *V-22 Osprey*, 08 Feb 2006, Globalsecurity.org, http://www.globalsecurity.org/military/systems/aircraft/v-22.htm
3. *USMC Attributes Osprey Crash to Software, Hydraulic Failure*, May 2001, Navy League of the United States, http://findarticles.com/p/articles/mi_qa3738/is_200105/ai_n8942867/
4. S. Trimble, *V-22 Program Grounds Fleet Citing Hydraulic Line Defects*, V22 Osprey Web, 10 Mar 2003, Department of the Navy, http://www.navair.navy.mil/v22/index.cfm?fuseaction=news.detail&id=46
5. *V-22 Osprey Hydraulic System-Report No. D-2002-114(PDF)-Project No. D2001LA- 0124.000*, V-22 Osprey Hydraulic System, 24 June 2002, Department of Defense, http://www.dodig.mil/Audit/reports/fy02/02114sum.htm
6. H. Keeter, *Navy Sacks V-22 Hydraulic Tubing Supplier*, V22 Osprey Web, 10 Mar 2003, Department of the Navy, http://www.navair.navy.mil/v22/index.cfm?fuseaction=news.detail&id=47
7. *Impulse Testing of Hydraulic Tubing and Fittings, S-N Curve*, SAE, Aerospace Standard AS4265, 2004, p 1–6
8. ATI Wah Chang Data Sheet, 2008
9. M.J. Donachie, *Titanium: ATechnical Guide*, 2nd ed., ASM International, 2000, p 1, 159, 160
10. C.E. Forney and S.E. Meredith, *Seamless Tubing Engineering Guide*, 3rd ed., Sandvik Special Metals Corporation, Washington, 1990, p 5, 16
11. A.L. Helbert, X. Feaugas, and M. Clavel, The Influence of Internal Stresses on the Fracture Toughness of α/β Titanium Alloys, *Metall. Mater. Trans. A*, 1999, **30**, p 2853–2863
12. O. Strehlau, *Introducing Cold Pilger Mill Technology: An Overview of the Equipment and Process*, 11 July 2006, TheFabricator.com, http://www.thefabricator.com/article/tubepipeproduction/introducing-cold-pilger-mill-technology
13. H.R. Salimijazi, T.W. Coyle, and J. Mostaghimi, Vacuum Plasma Spraying: A New Concept for Manufacturing Ti-6Al-4V Structures, *JOM*, 2006, **90**, p 50–56
14. R. Boyer, G. Welsch, and E.W. Collings, Ed., *Materials Properties Handbook: Titanium Alloys*, ASM International, Materials Park, OH, 1998, p 3–31
15. J. Kallend, U.F. Kocks, A.D. Rollett, and H.R. Wenk, Operational Texture Analysis, *Mater. Sci. Eng. A*, 1991, **132**, p 1–11
16. R.W. Hertzberg, *Deformation and Fracture Mechanics of Engineering Materials*, John Wiley & Sons, New York, 1996
17. D.R. Askeland and P.P. Phule, *The Science and Engineering of Materials*, 5th ed., Thomson Canada Limited, Toronto, 2006, p 521–522
18. J.E. Gordon, *Science of Structures and Materials*, Scientific American Library, Distributed by Freeman, New York, 1988
19. D.J. Maykuth, *Residual Stresses, Stress Relief, and Annealing of Titanium and Titanium Alloys*, Defense Metals Information Center, Columbus, OH, 1968